Zeitschrift: IABSE proceedings = Mémoires AIPC = IVBH Abhandlungen

Band: 5 (1981)

Heft: P-44: Evolution up to failure of continuous prestressed concrete bridge decks

Artikel: Evolution up to failure of continuous prestressed concrete bridge decks

Autor: Aparicio, A.-C. / Arenas, J.-J.

DOI: https://doi.org/10.5169/seals-35888

Evolution up to Failure of Continuous Prestressed Concrete Bridge Decks

Sollicitations jusqu'à la ruine d'un pont continu en béton précontraint

Die Beanspruchung bis zum Bruch eines durchlaufenden vorgespannten Brückenträgers

A.-C. APARICIO
Associated Prof.

J.-J. ARENAS
Professor of Bridges

Escuela Técnica Superior de Ingenieros de Caminas,
Santander, Spain

SUMMARY

This work consists of a non-linear analysis of continuous prestressed concrete bridge decks in which the actual behaviour of structural material is simulated through the moment-curvature relationships of the prestressed sections. In order to obtain these diagrams, the real behaviour of the materials (concrete and steel) is taken into account, including the effects of cracking and the presolicitation of the active steel which produces a shift of the moment-curvature origin of the diagram corresponding to every section. A method for predicting the bending law evolution with increasing intensity of loads, up to deck failure by bending, is therefore outlined.

RÉSUMÉ

Ce travail porte sur une méthode d'analyse non linéaire des tabliers continus en béton précontraint, en simulant le comportement réel des matériaux au moyen des relations moment/courbure des différentes sections. Pour ce faire, on tient compte des lois réelles constitutives du béton et de l'acier, en incluant la fissuration et le déplacement de l'origine des diagrammes moment/courbure produit par la présollicitation de la précontrainte. On décrit en lignes générales une méthode pour connaître l'évolution des lois des moments avec charges croissantes jusqu'à la rupture du tablier.

ZUSAMMENFASSUNG

Bei dieser Arbeit handelt es sich um eine Methode der nichtlinearen Analyse von durchlaufenden Brückenträgern aus Spannbeton, wobei das Verhalten der Baustoffe durch Momenten-Krümmungs-Diagramme für die verschiedenen Schnitte simuliert wird. Um diese Diagramme aufzustellen, berücksichtigt man die Spannungs-Dehnungs-Funktion des Betons und des Stahles einschliesslich der Auswirkungen der Rissbildung und der Verschiebung des Koordinatenursprunges infolge der Vorspannung.
Es werden die Grundzüge einer Methode dargelegt, die die Entwicklung des Momenten-Diagrammes bei wachsenden Belastungen bis zum Biegebruch im voraus bestimmten.

1.- INTRODUCTION

The prestressed concrete continuous bridge-decks are usually analyzed at the service state, where materials present elastic and linear behaviour. The superposition principle is valid and the internal forces due to the prestressing or thermal gradient or differential settlement are easily calculated in the same way as any other external loading case.

In order to check security at the ultimate limit state, we usually amplify the internal force values corresponding to service state (elastic and linear analysis) by the appropiated load factors, verifying that in any section the equation:

$$Sd < Ru, \text{ is satisfied.}$$

This procedure ignores the change in real behaviour of the continuous deck, where for increasing load intensity, more or less extended zonal cracking appears, while the non-linear behaviour of the constitutive materials (concrete and steel) is accentuated. In particular, the usual practice of amplifying or reducing the hyperestatic service-level efforts due to prestressing, or to thermal gradient or differential settlement, as an attempt to find the corresponding real values in the ultimate limit state, has no physical meaning and does not allow the designer to estimate the true safety margin against failure of the sections and, therefore, of the whole deck.

This work is an attempt to approximate to the knowledge of the true evolution of a prestressed concrete continuous deck under any system of increasing loads, where the actual behaviour of the structure is simulated through the moment-curvature diagrams of a sufficient number of sections in each span. It is a non-linear analysis method, where the superposition principle is no longer valid, which gives us the resulting bending moment law for any combination of external loads and imposed deformations, not equivalent to the sum of the bending laws corresponding to each of the involved load cases separately.

Our final objective is to estimate the value of the amplifying load-factor γ, which, applied to a certain loading-case, produces the deck failure, i.e. at least in one section the acting moment M_d equals the ultimate resistant moment:

$$M_d = M_{uR}$$

2.- BASIC ASSUMPTIONS

2.1.- Shear deformation is neglected. This means:

i) In longitudinal bending we consider as effective the whole width of flanges and cantilevers, i.e, no shear lag is taken into account.

ii) No shear deformation is considered in the web. Concrete diagonal cracking, if it exists, is assumed to be sufficiently controlled through closely spaced stirrups.

iii) In the same way, the ultimate shear capacity in the webs and flanges, is great enough compared to the ultimate bending resistance.

2.2.- Tensile strength of concrete has been taken into account for the evaluation of the cracking bending moment. However, the "tension-stiffening" effect has been neglected as we are dealing with post-tensioned concrete, with tendons in ducts bonded by injection.

With the above basic assumptions we may assume that the moment-curvature diagram of any section accurately represents the real constitutive law of the structural material.

3.- MOMENT-CURVATURE DIAGRAM OF ANY PRESTRESSED SECTION

Its determination is based on the following points:

i) We consider that the moment-curvature diagram represents the behaviour of the prestressed sections once we know its "permanent stress state", which is due to the total dead weight moment plus the prestress effects after losses. We can obtain, through an elastic calculus, the resulting bending moment ($M = M_{g1} + M_{g2} + M_{HP}$) and its corresponding negative section curvature $(1/r)_1$, plotted as point 1 in figure 1.

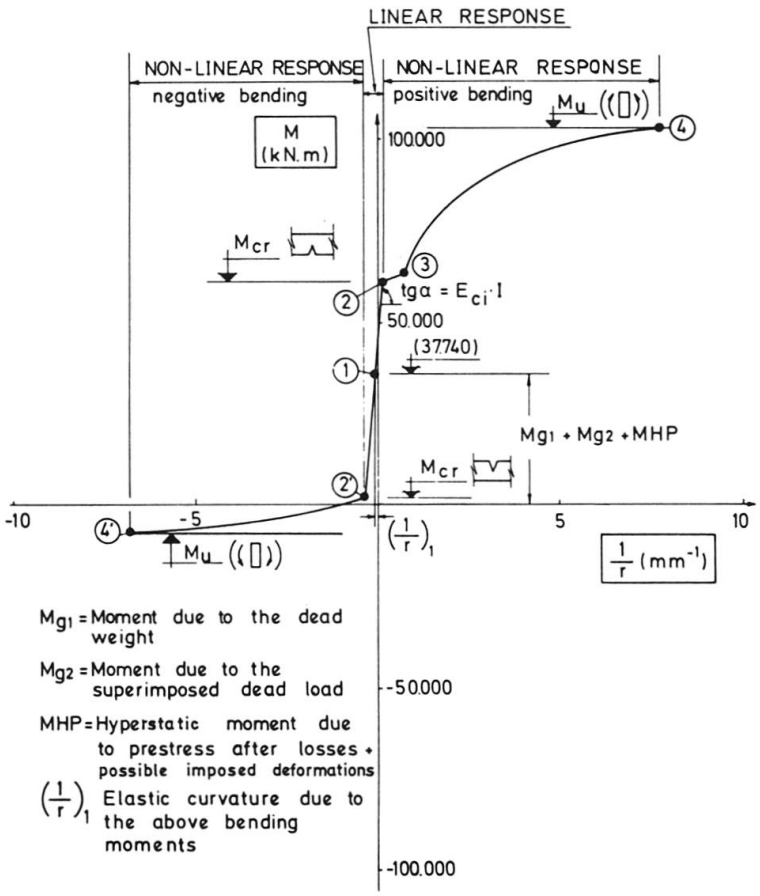

FIGURE 1.-Moment - curvature relationship of a prestressed cross - section (Corresponding to cross section [2-6] of the example in figure 6)

ii) Any increase or reduction of the bending moment acting on the section leads to a linear response, until cracking of the section is reached. Points 2 and 2' represent positive and negative cracking bending moments.

iii) For bending moments greater in absolute value than the cracking moment, the section's response is calculated through its equilibrium and compatibility conditions, on the hypothesis of planar deformation and considering the constitutive laws of the actual materials, i.e. concrete and active and pasive steels.

In figure 1, we represent the (M - χ) diagram of the section (2.6) at the middle of the central span of the bridge indicated in figures 4 and 5. One may observe the linear segment betwen points of cracking (linear response), and the two curved lines up to failure, 4 and 4', under positive and negative resulting external bending moment. It is worthwhile underlining the theoretical slope discontinuity between points 2 and 3, according to the neglected tension-stiffening effect.

We must point out that on the Y asis we represent the total external moments, i.e. the moment due to external load and support reactions, thus including the hyperestatic moment due to prestress and any other moment introduced by any imposed deformation. On the X axis we represent the absolute curvature of the section due to all the above effects plus the isostatic prestress bending moment. Under such conditions, one may observe the fact that, generally, the diagram does not pass through the origin of coordinates.

A detailed procedure for determining the "mechanical surface" (Axial force-Bending moment-Associated curvature) of any arbitrary reinforced concrete section may be seen in ref. {3}. Its extension to prestressed sections is included in ref. { 1 }.

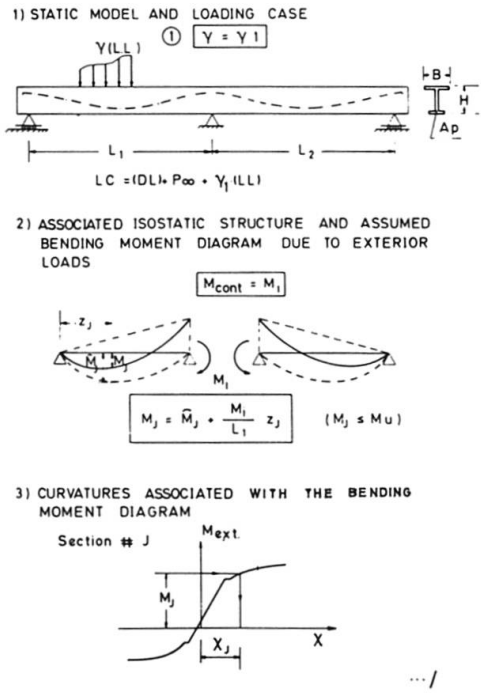

FIGURE 2a

4.- CONTINUOUS DECK METHOD OF ANALYSIS

The method of analysis stated follows a flexibility procedure, choosing as redundants the continuity bending moments over intermediate supports. For the solution, an iterative technique has been followed.

In figure 2, a chart of the analysis method is presented, particularized for a case of a two span beam, summarising in the next paragraph the basic steps of the procedure.

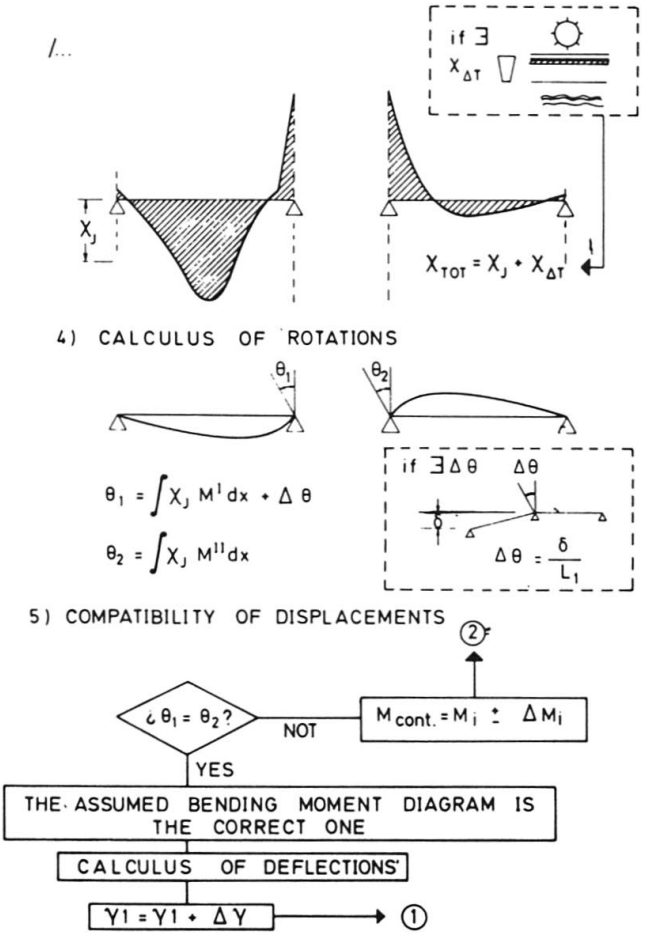

FIGURE 2b.- General chart of non-linear analysis of continuous prestressed concrete beams

Once geometrically and mechanically defined, the beam will be studied for a certain loading case, following its evolution up to failure as the load intensity increases.

For a certain level of load stage ($G + \gamma Q$), we know through equilibrium conditions the bending moment diagrams in the Associated Isostatic Structure (succesion of simple spans). If we assume an aproximate value for the continuity bending moments, we can calculate the existing bending in each span under such load level and the assumed values of redundants. Once the bending moment-curvature relationship at every section have been stated, we may obtain the existing curvature in each section, J, under the already known bending moment acting on it, M_J.

The curvature laws corresponding to that load level in each span is thus determined. Through the Mohr theorems, it is easy to calculate the rotations at the ends of each span of the associated isostatic structure.

The compatibility condition requires that both spans abutting on the same intermediate support have equal rotations. If this happens, the assumed value for the follow-up bending moment, M_i, is the right one. If not so, what normaly happens with non-linear structural behaviour is that the follow-up moments must be modified, substituting M_i by another value, M_{i+1}, in the next iteration cycle.

When the associated curvatures due to the bending moment law lead to the same rotations at the common support to both spans, the compatibility condition is fulfilled and, consequently, the assumed bending moment law is the correct one for this load level.

By gradually increasing the external live load amplifier coefficient, γ, we obtain for each load level the corresponding bending moment law.

The failure will be reached when the intensity of the load, $G + \gamma Q$, is such that, in at least one section, the resulting bending moment equals its ultimate moment.

In the preceding paragraphs the gravitational action treatment has been shown.

Prestressing, expressed as a predeformation of the sections, is directly reflected in the moment-curvature relationships, as we have seen before.

The temperature gradient action produces a change in the curvature of each section, being added to the curvature derived from the actuating bending moment.

A differential settlement implies a rotation in the Isostatic Associated Structure. The compatitility condition is expressed by equalizing, the total rotations, which are the sum of the rotation derived from this settlement plus the integrals of the curvatures.

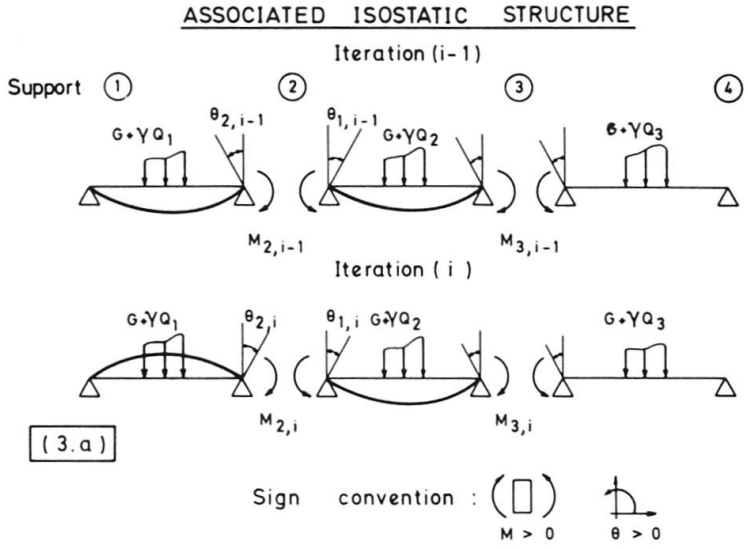

(Bending moment - Rotation) Diagram at Support 2

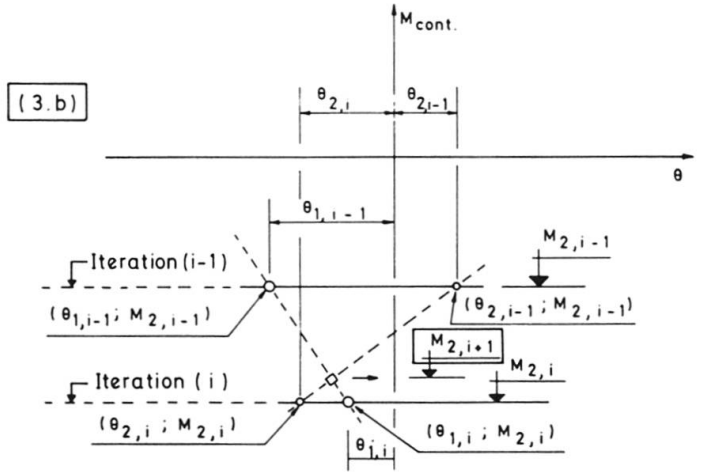

FIGURE 3.- Iteration procedure for continuity bending moment determination

In figure 3, we indicate the iterative procedure for obtaining the continuity bending moments corresponding to a certain load level. Focusing our attention on support number 2 (fig. 3a), we may observe (fig. 3b) how for a value, $M_2 = M_{2,\,i-1}$, the rotations calculated through span curvatures are $\theta_{1,\,i-1}$ and $\theta_{2,\,i-1}$, which are not equal. A new iteration with a value, $M_2 = M_{2,i}$, leads to rotations $\theta_{1,i}$ and $\theta_{2,\,i}$, which are neither equal. Through linear interpolation we obtain a new value for M_2, $M_2 = M_{2,\,i+1}$, continuing until a practical convergence is reached.

The rate of convergence of this method is variable, depending on the bridge design and loading case, but, generally, 3 to 11 cycles have been found sufficient.

A computer program, written following the above mentioned techniques, has yielded results which in comparison with, among others, the experimental results of G. MACCHI (C - 2 beam, ref. {2}), surpass its ultimate measured load by only 1%. Therefore, this program has been used for the study of the evolution up to failure of several bridges already in use designed by the Authors. In this paper we include only the results concerning one of these bridges.

5.- DESCRIPTION OF A REAL BRIDGE ANALYZED

We refer to the "Cuzco-Barajas" Bridge, which spans the M-30 motorway in Madrid (Spain). It is a three span continuous prestressed concrete deck, of (43 + 48 + 43) m. and 30 m. wide, with constant depth equal to 1,70 m. (fig. 4). Its typical cross section, two celular girders connected by a central slab, is shown in figure 5.

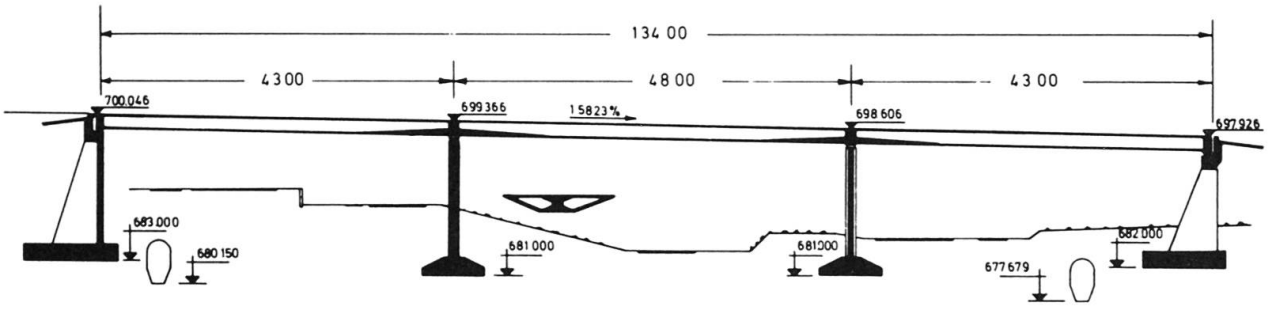

FIGURE 4.- "Cuzco - Barajas" Bridge over motorway M-30 in Madrid (Spain). Longitudinal section.

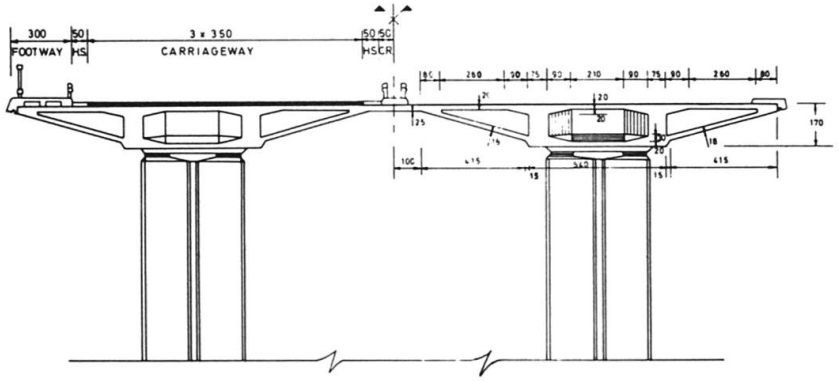

FIGURE 5 - "Cuzco - Barajas" Bridge General cross - section

The prestress consists of 20 tendons, 5 by main web, composed of 36 strands, 0.6" diameter, anchored at both bridge abuttments, with 136 meters length. Its ultimate breaking load is equal to 182360 kN (f_{pm} = 1730 N/mm^2), and the initial prestressing load was 145880 kN (1384 N/mm^2). The bridge is designed in Class I (total prestress).

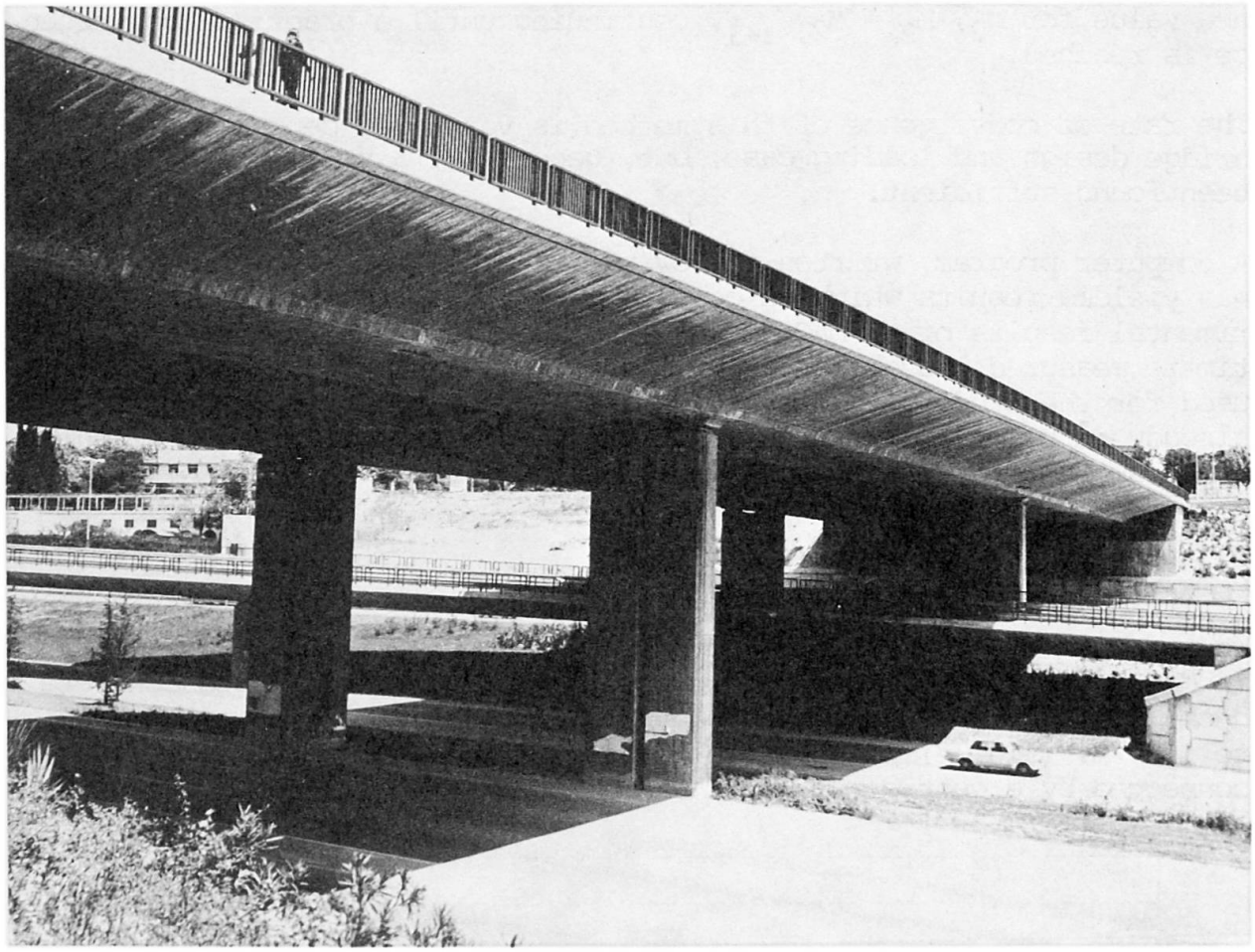

Photograph 1

In photograph 1 one may see an aspect of the finished bridge. More information about it may be found in ref. {4} .

6.- RESULTS OF THE THEORETICAL ANALYSIS.

Considering in the analysis, eleven equally spaced sections per span, the following results have been found:

In figure 6 the evolution of the bending moments at three critical sections of the deck, for loading case 1, with increasing live load (γ factor) is shown. Particularly, one may observe:

a) - From γ = 0 up to γ = 1.5 the behaviour of the continuous beam, without cracking at any section, is linear.

b) - For $\gamma = 1.5$ the cracking moment value is reached at section (2.6), as may be seen in the corresponding moment-curvature diagram on the right side of the figure.

c) - Consequently, the relative stiffness of the central span is reduced and, for increasing γ, the support (2.1) bending moment increases faster than the corresponding linear value, while, logically, the central section (2.6) bending moment increases more slowly.

d) - For γ equal to about 3, the cracking of the support section (2.1) takes place and the above tendency is slightly changed.

e) - When $\gamma = 4$, the cracking of section (1.8), which implies the beginning of a state of generalized cracking of the zone of lateral spans near the intermediate supports, again reverses the increasing tendency of the moments.

f) - Finally, when $\gamma = 5.24$, the bending moment at central section (2.6) reaches the value of the ultimate response moment, and we accept that for this level of live load the continuous deck collapses.

We observe the increase of load carrying capacity through the non-linear analysis according to the possibility of redistribution of bending moments of the deck. With linear analysis, we find $\gamma_{col} = 4.54$, while the non-linear gives $\gamma_{col} = 5.24$, with 16% of load carrying capacity increase.

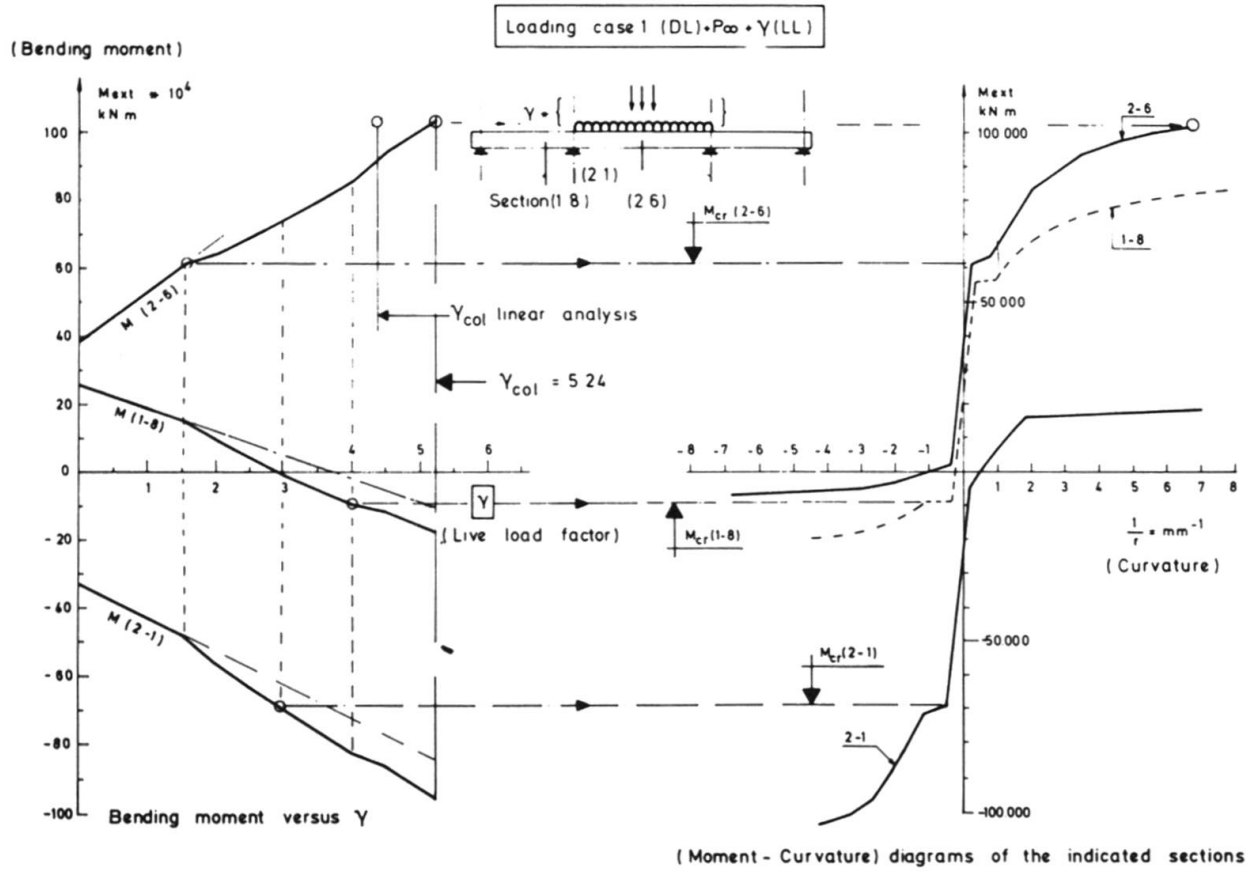

FIGURE 6.- Loading case 1. Evolution of bending moments at sections (1 8), (2 1) and (2 6) with increasing live load-factor γ

Such final state is described in figure 7. Here one may see the cracked and the uncracked deck zones, the final bending moment law (M_{col}), the collapse of the central section (2.6) and the existing small margin of resistant capacity at the section of supports (2.1) and at the intermediate critical section of lateral span (1.8). We observe that more ductility (increase in the curvature of the sections for its ultimate response bending moment) in the center bridge section would allow a complete plastic adaptation of the continuous deck, with the simultaneous collapse of the lateral span critical sections, and the overall result of a slight increase in the γ ultimate live-load factor.

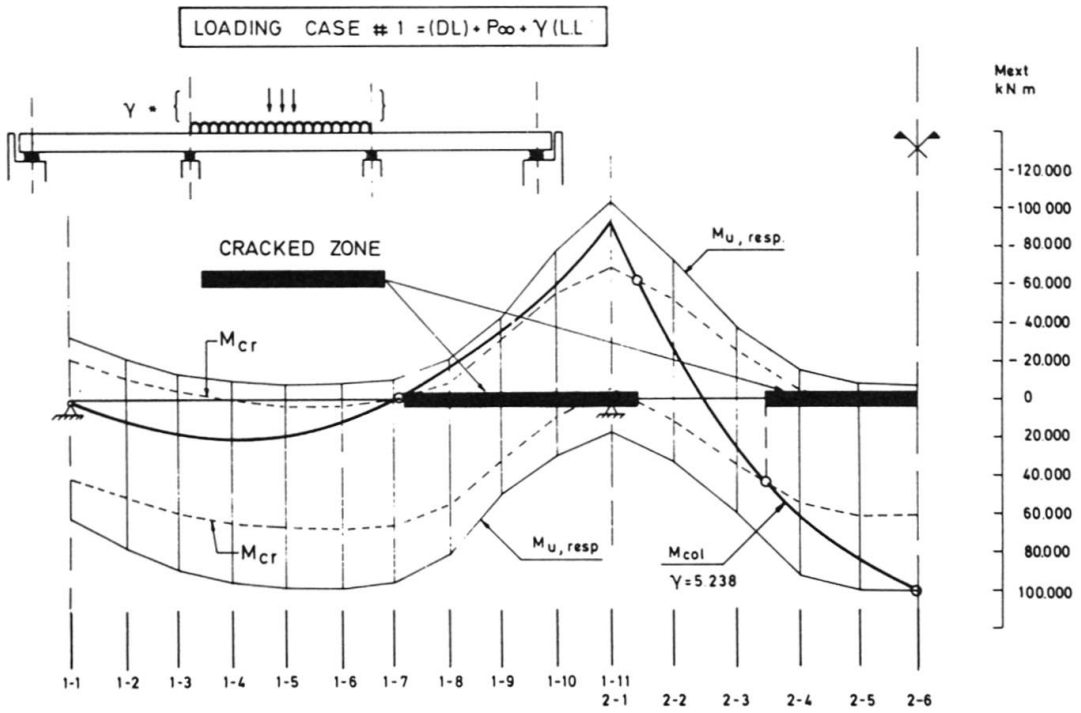

FIGURE 7.- Final state of the continuous deck at collapse, for loading case 1

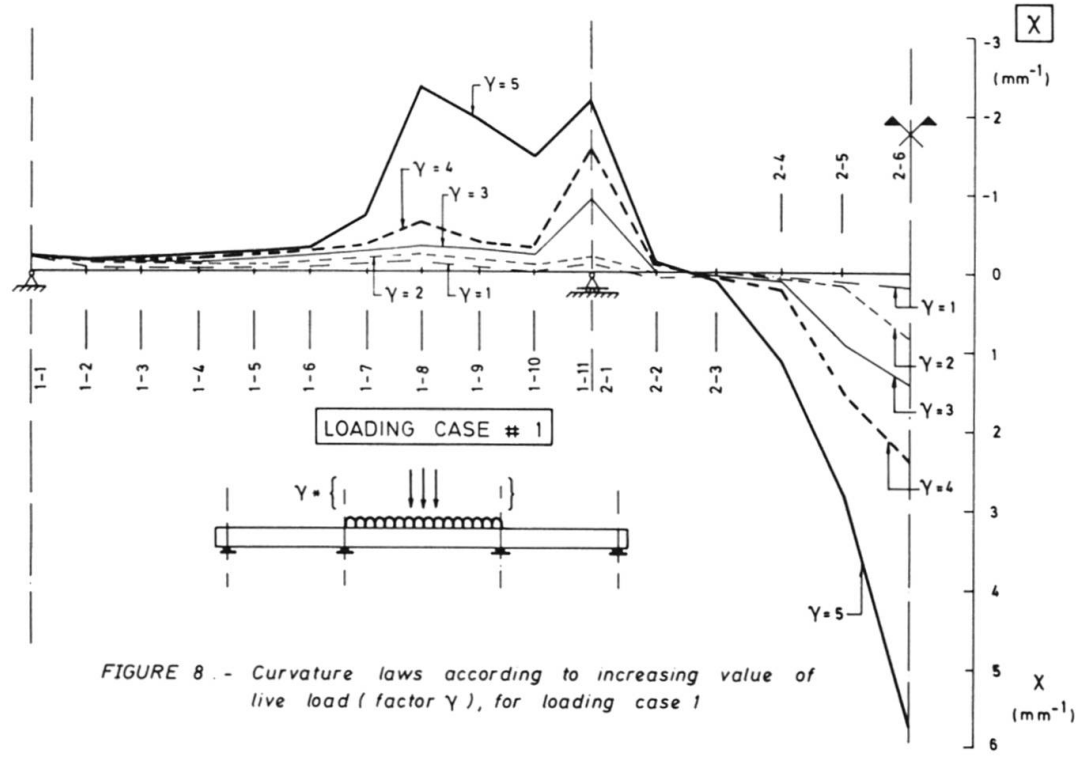

FIGURE 8.- Curvature laws according to increasing value of live load (factor γ), for loading case 1

In figure 8 we represent the existing curvatures along the deck for increasing values of the γ live-load factor. One may observe the beginning of cracking in the central zone for $\gamma = 2$, the cracking of the support zone for $\gamma = 3$, and the generalized cracking of the side zone of lateral span near the intermediate support for $\gamma = 5$, in the proximity of deck collapse. For any value of γ, one may estimate the equality of rotations of both span abuttments through the corresponding curvature law. This figure illustrates how the concentrated hinge procedures of analysis are far from reality in the case of prestressed concrete continuous beams.

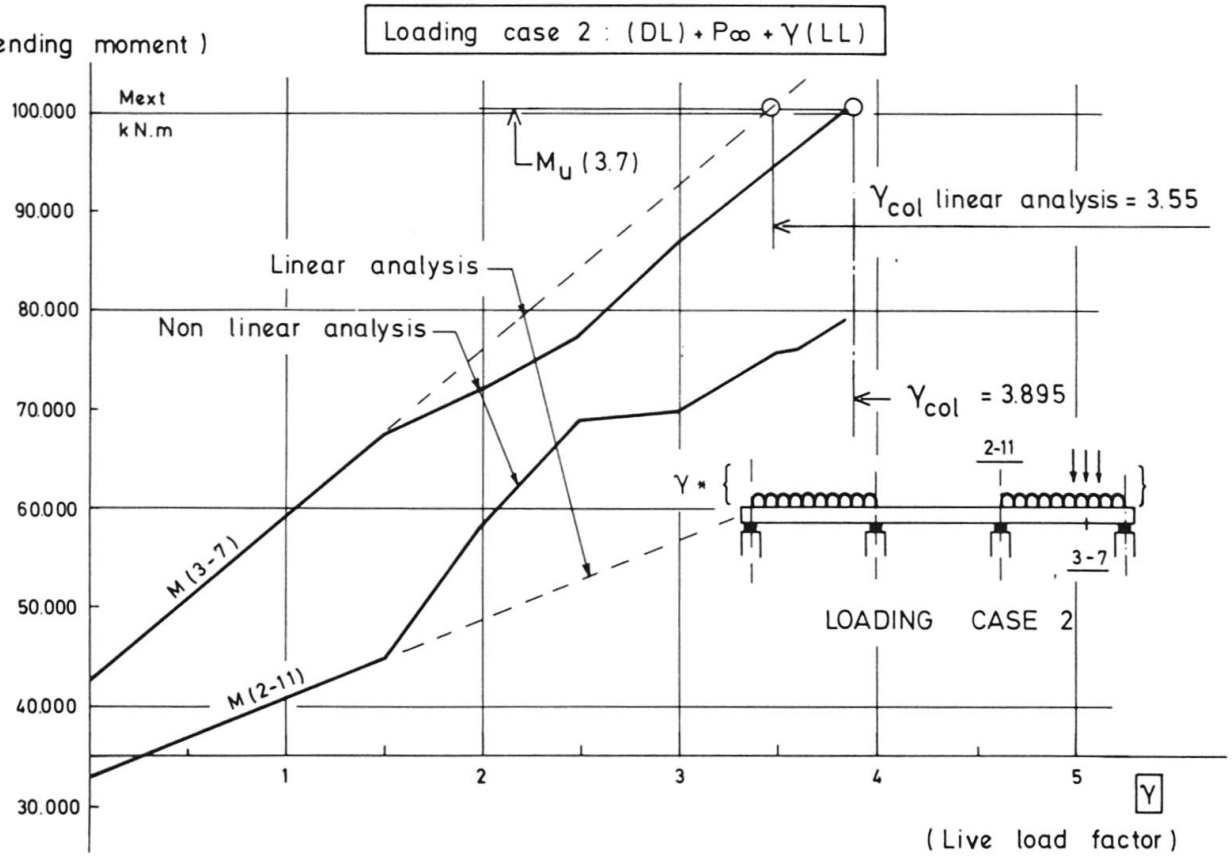

FIGURE 9.- Loading case 2. Evolution of bending moments at critical sections with increasing live load factor γ.

Loading-case 2 is shown in figure 9, where the evolution of the bending moment at support section (2.11) and intermediate mainly loaded lateral span section (3.7) with increasing value of the live-load factor γ may be observed. For $\gamma = 1.5$ the (3.7) section cracks and for $\gamma = 2.5$ cracking appears at support section (2.11). The collapse of the deck occurs when section (3.7) reaches its ultimate bending resistance, while the support section bears only 78% of its ultimate bending moment. This may be seen in figure 10 where the bending moment collapse law, as well as the corresponding curvatures along the deck, are represented. Here one may observe the generalized cracking zones: Lateral right span and right side of central span.

The increase in maximun load carrying capacity yielded by the non-linear analysis relative to the linear capacity is of 9.7%. The plastic adaptation is nearly total, as section (2.8) bending moment is very close to its ultimate response value.

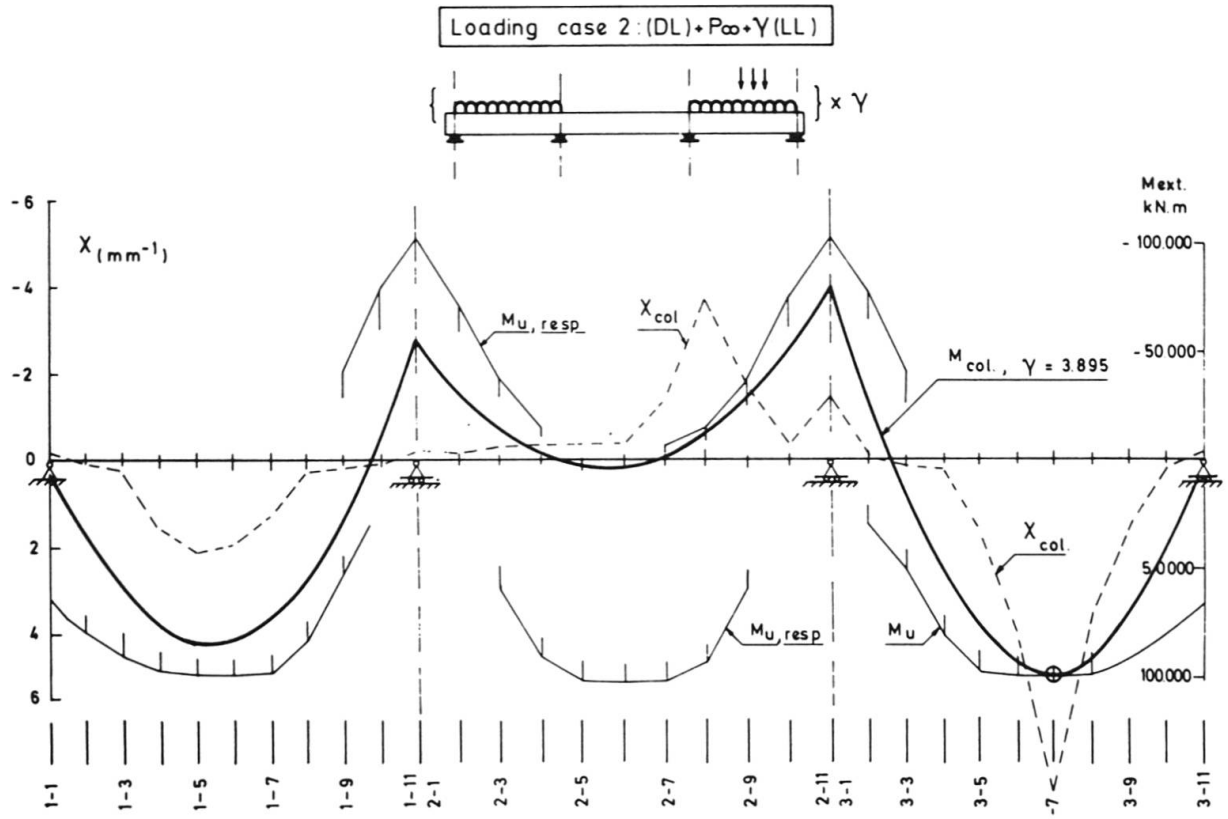

FIGURE 10.- Loading case 2. Final state at collapse of the deck

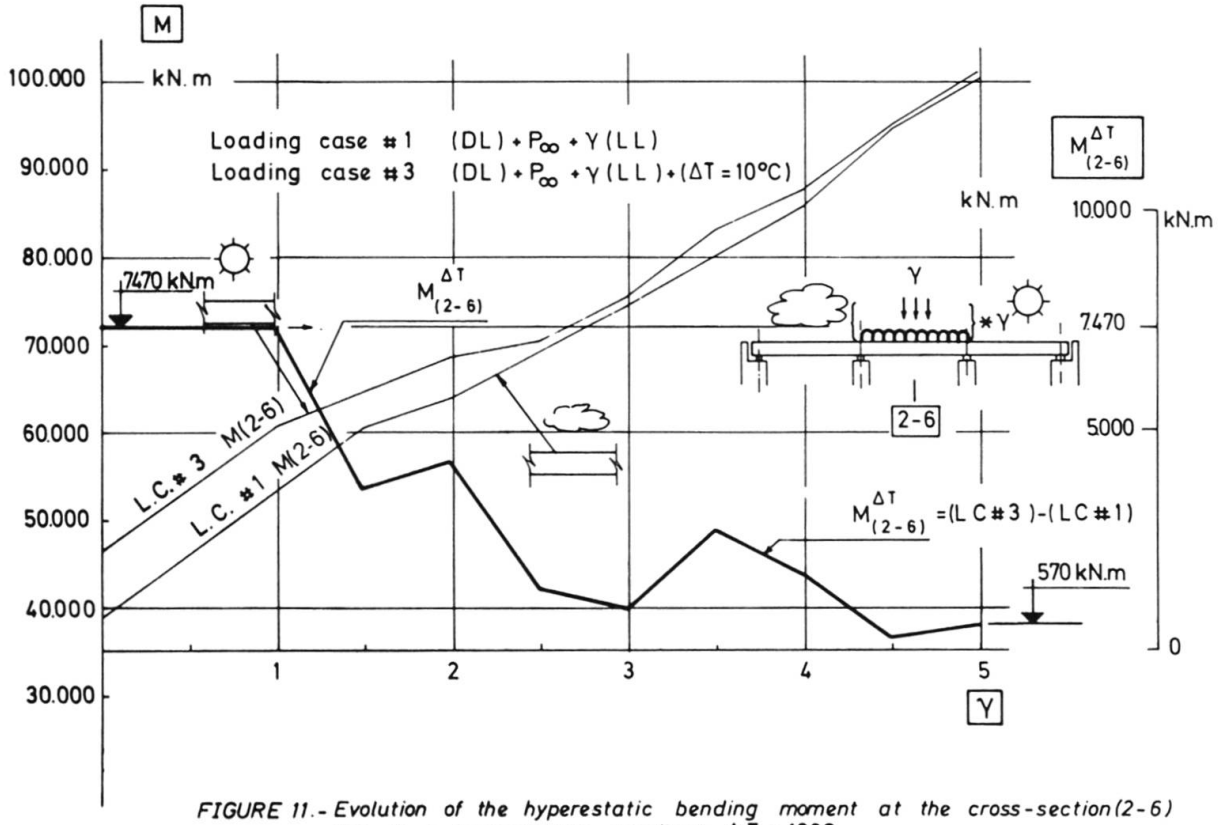

FIGURE 11.- Evolution of the hyperestatic bending moment at the cross-section (2-6) due to a temperature gradient, ΔT = 10°C

In figure 11, we represent the evolution of the bending moment at the center bridge (2.6) section for loading-case 1 described above, and loading-case 3, sum of the first and a thermal linear gradient ΔT = 10°C between top and bottom fibers, as the live-load factor γ increases. The difference between the values of both curves represents the "pure" effect of the thermal gradient, which is drawn in the same figure and here one may observe its tendency to vanish when the live-load factor increases. In this way, an initial elastic value of 7470 kN.m for M(2.6) due to thermal gradient decreases up to 570 kN.m at the proximity of the deck collapse. The ultimate live-load factor reaches a value of γ = 5.22 which compared to the value of 5.24 correspondign to loading-case 1 shows the very small influence of the imposed deformation in the maximun load carrying capacity of the deck.

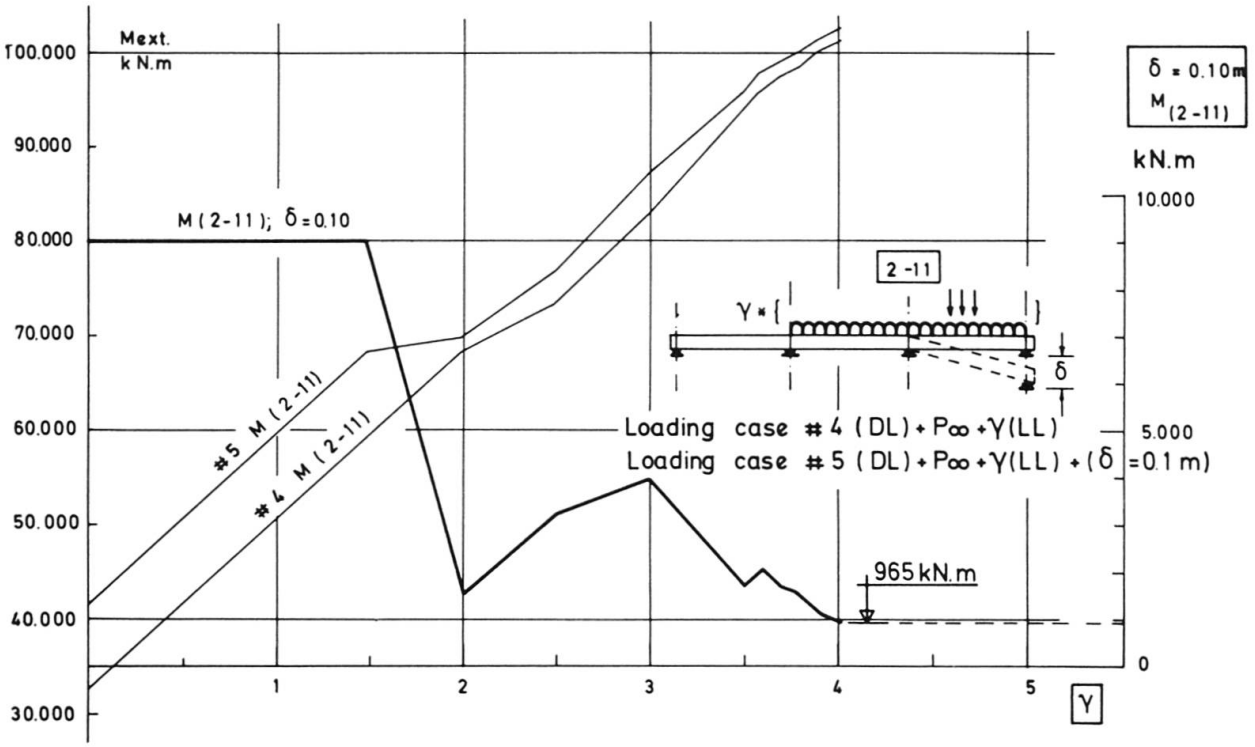

FIGURE 12 . - Evolution of the bending moment at the support cross-section (2.11), due to an abuttment settlement, δ.

The same tendency for the case of differential settlement of an abuttment may be observed in figure 12. From an initial value, in the elastic range of M(2.11) = -8920 kN.m, the "pure" effect of the abuttment settlement is reduced to -965 kN.m at the collapse of the deck, and the ultimate live-load factor changes from 4.12 for the loading-case 4, to 4.05 when the differential settlement occurs.

The tendency to vanish for the imposed deformation bending moments when external load increases has been verified by the Authors in the analysis of other real bridges. On the contrary, the tendency for the increase in the external load carrying capacity is not so general. For another real bridge with marked variation of depth, the Authors have found for some loading-case, reductions up to 8% in comparison with the elastic load carrying capacity (ref. { 5 }).

REFERENCES

1 APARICIO, A.C.:

Estudio de la evolución hasta la rotura por solicitaciones normales de tableros continuos de puentes de hormigón armado o pretensado. (Study on the evolution up to the failure by bending of continuous decks of reinforced or prestressed concrete bridges). Ph. D. Thesis, Universidad de Santander, Spain, 1980.

2 MACCHI, G.:

Etude expérimentale de poutres continues précontraintes dans le domaine plastique et á la rupture.
FIP, Amsterdam, 1955. Session III, Paper nº 2.

3 ARENAS, J. J.:

Cálculo de soportes de hormigón armado en teoría de segundo orden. (Design of reinforced concrete columns including second order effects).
Editores Técnicos Asociados. Barcelona, 1980.

4 ARENAS, J. J., APARICIO, A. C.:

El puente del Eje Cuzco-Barajas del enlace de Santamarca en la Autopista de la Paz, en Madrid.
Hormigón y Acero nºS 130, 131, 132, ATEP - Instituto E. Torroja de la Construcción y del Cemento. Madrid, 1979.

5 ARENAS, J. J., APARICIO, A. C.:

El paso superior sobre la Autovía de los Pirineos en la ACTUR Puente de Santiago de Zaragoza.
To be published in Hormigón y Acero, ATEP, Instituto E. Torroja, Madrid.